Journal of Alloys and Compounds 509 (2011) 7968–7972

Contents lists available at ScienceDirect

Journal of Alloys and Compounds

journal homepage: www.elsevier.com/locate/jallcom

Synthesis and visible-light photocatalytic activity of $NdVO_4$ nanowires

Jing Xu[a,b], Chenguo Hu[a,*], Gaobin Liu[a], Hong Liu[c], Guojun Du[c], Yan Zhang[a]

[a] Department of Applied Physics, Chongqing University, Chongqing 400044, PR China
[b] Chongqing University of Science and Technology, Chongqing 401331, PR China
[c] State Key Laboratory of Crystal Materials, Shandong University, Jinan 250100, PR China

ARTICLE INFO

Article history:
Received 2 December 2010
Received in revised form 11 May 2011
Accepted 13 May 2011
Available online 19 May 2011

Keywords:
$NdVO_4$ nanowires
Composite-molten-salt method
Photocatalytic activity

ABSTRACT

$NdVO_4$ nanowires are synthesized by a simple composite molten salt method. Scanning electron microscopy, transmission electron microscopy, X-ray diffraction spectrum, energy dispersive spectrometry and UV–vis spectrum are used to characterize the structure, morphology and composition of the sample. The results show that the product is of tetragonal phase $NdVO_4$ nanowires which are connected together in bases, rooted in one center, with typical diameters of 100 nm and lengths up to 3 μm. The UV–vis spectrum shows that $NdVO_4$ nanowires have four strong absorption peaks from the UV to near infrared region. The photocatalytic degradation of Rhodamine B (RhB) and methyl orange under visible light irradiation using the $NdVO_4$ nanowires are also investigated. Excellent catalytic degradation activity of RhB observed suggests possible applications for organic pollutant treatment under visible light irradiation. The electron density states of the $NdVO_4$ were calculated with the Vienna *ab initio* simulation package. The results of these simulations were used to form a description of the observed light absorption and photodegradation properties of $NdVO_4$ nanowires.

© 2011 Elsevier B.V. All rights reserved.

1. Introduction

Photocatalysis is a clean technology in the treatment of a variety of contaminants. The low cost, high photoactivity and recyclable features of TiO_2 makes it one of the most commonly used photocatalysts [1]. However, TiO_2 shows photocatalytic activities only in the UV region and can harvest a small fraction (<5%) of the solar irradiation due to its relatively large band-gap (about 3.2 eV) [2–4]. Therefore, development of visible light active photocatalysts to efficiently utilize solar energy is both an important and challenging research field [5–7]. The visible light photocatalytic activity of TiO_2 nanotubes [2], nanoparticles [3,8] and hollow spheres [4] have all been enhanced by doping with Nd, owing to the increased visible light absorption from the narrowed band-gap. In addition, a large number of un-doped semiconductor photocatalysts have been developed demonstrating absorption in the visible light region. These new photocatalysts including Ag_3VO_4 [9] and $BiVO_4$ [10,11] have demonstrated efficient photocatalysis under visible light irradiation. Neodymium is a rare earth element with luminescent and photocatalytic properties due to the transitions of 4f electrons under visible light irradiation [12,13]. $NdVO_4$ nanorods and nanoparticles have been synthesized and the catalytic properties have been investigated under UV irradiation [14,15], but there is no report on their catalytic properties under visible light irradiation.

In this paper, we have reported for the first time the synthesis of $NdVO_4$ nanowires by the composite molten salt method (CMS). The CMS approach is a new strategy that provides a one-step, low-cost, convenient, environmentally friendly, and scalable production route for synthesizing nanostructures of functional materials [16]. The catalytic degradation activity of the $NdVO_4$ nanowires to Rhodamine B (RhB) is investigated. To the best of our knowledge, this is the first report on the catalytic degradation activity of RhB by using $NdVO_4$, and the first report of $NdVO_4$ catalytic activity under visible light irradiation.

2. Experimental

$NdVO_4$ nanowires were prepared by the CMS method. All the chemicals were purchased from Chongqing Chemical Company, and used without further purification. In a typical procedure: (1) 9 g mixed nitrate ($LiNO_3/KNO_3$ = 1:2) was put in a 25 mL teflon vessel. (2) 1 mmol $NdCl_3{\cdot}6H_2O$ and 1 mmol V_2O_5 were added in the vessel. (3) The vessel was sealed and put in a furnace preheated to 200 °C. (4) After reacting for 24 h, the vessel was taken out and allowed to cool to room temperature. (5) The greenish product obtained was washed with deionized water and ethanol several times.

The crystal phase of the product was characterized by a BDX320 X-ray diffraction instrument equipped with Cu Kα radiation (λ = 1.5418 Å). A scanning rate of 4°/min was applied to record the spectrum over range of 2θ, 20–70°. The morphology and size of the products were analyzed using a scanning electron microscope (TESCAN VEGA2) equipped with an energy dispersive X-ray spec-

* Corresponding author. Tel.: +86 23 65104741; fax: +86 23 65111245.
E-mail addresses: hucg@cqu.edu.cn, hu.chenguo@yahoo.com (C. Hu).

0925-8388/$ – see front matter © 2011 Elsevier B.V. All rights reserved.
doi:10.1016/j.jallcom.2011.05.051

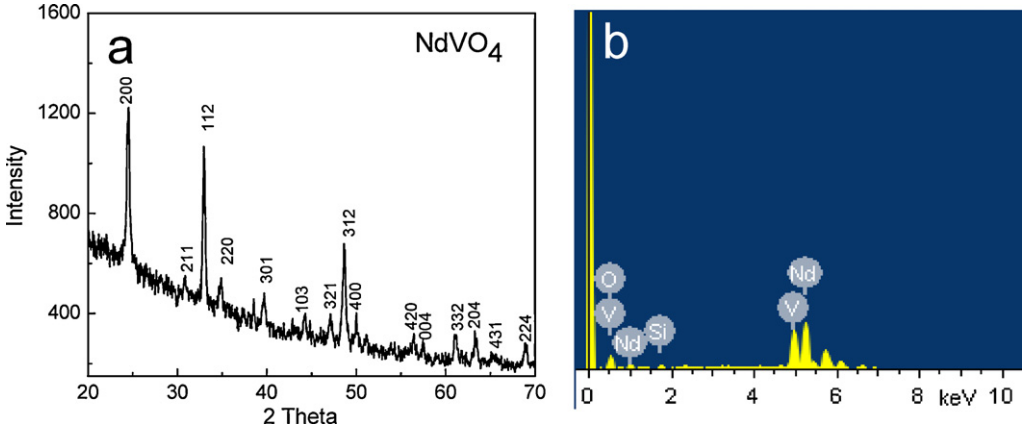

Fig. 1. XRD pattern (a) and the energy dispersive spectrum (b) of the $NdVO_4$ nanowires.

troscopy (EDS), and transmission electron microscope (TEM). To examine the band gap of the samples, UV–vis absorption spectrum of the sample on quartz slices was measured by U-4100 UV–vis–NIR spectrophotometer under normal incidence light.

The degradation of RhB was performed by a simulated sunlight instrument (CHF-XM-500 W). The change in the RhB concentration was monitored using a UV–vis spectrophotometer (Hitachi U-4100). 20 mg of the $NdVO_4$ nanowires were dispersed in 100 mL solution with 0.01 mmol/L RhB in a glass beaker. Before illumination,

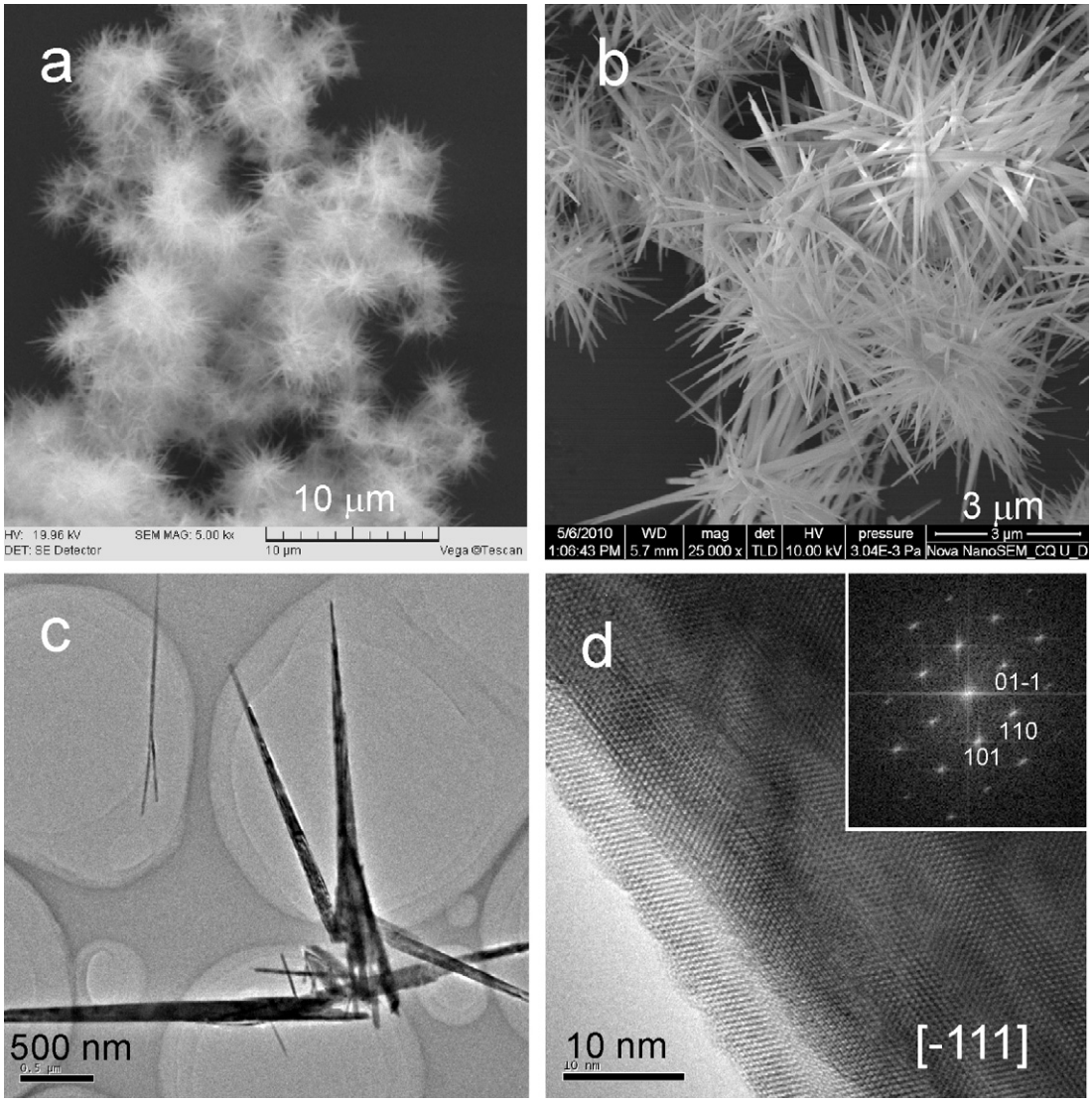

Fig. 2. SEM images (a and b), TEM image (c), selective area electron diffraction pattern (inset) and HRTEM image (d) of the $NdVO_4$ nanowires.

the suspension was magnetically stirred for 1 h in the dark to ensure adsorption equilibrium of RhB on the surface of the sample.

3. Results and discussion

XRD patterns in Fig. 1a demonstrate a crystallized product. The diffraction peaks for the sample were indexed as the tetragonal structure of $NdVO_4$ (JCPDS: 15-0769, S.G. $I4_1/amd(141)$), with lattice constants of $a = 7.33$ Å and $c = 6.44$ Å. Fig. 1b shows the energy dispersive spectrum (EDS) of $NdVO_4$ crystals, which confirms that the product is composed of three elements: Nd, V and O (the Si signal is from the substrate).

The SEM images (Fig. 2a and b) show that the sample is composed of nanowires with diameters of about 100 nm and lengths up to 3 μm connected together in groups at their bases. The TEM image (Fig. 2c) of the $NdVO_4$ sample further demonstrates their wire-like morphology and diameter of about 100 nm. HRTEM (Fig. 2d) suggests that the $NdVO_4$ nanowire is a single-crystalline, multi-layered structure with the layer plane orientation along [−1 1 1].

A possible formation mechanism of the $NdVO_4$ nanowires in the molten mixed salts is suggested. V_2O_5 and $NdCl_3{\cdot}6H_2O$ dissolve in the molten mixed nitrate solvent, and V_2O_5 is readily transformed to VO_3^- (or $V_4O_{12}^{4-}$) in the neutral solution. $NdVO_4$ nanoparticles are then formed by the reaction of VO_3^- with Nd^{3+} [13]. The small nanoparticles congregate to form large particles. According to the nucleation limit accumulation model, the supersaturation of the system significantly decreases because of the reactant exhaustion after the primary nucleation stage resulting in restrained nucleation. To reduce the high surface energy and the large surface curvature of the crystal nucleus, $NdVO_4$ crystal nuclei aggregate to form NdVO4 nanowires.

The UV–vis absorption spectrum of the $NdVO_4$ nanowires from 240 nm to 800 nm is shown in Fig. 3a. The spectrum shows distinctive absorption edges around 420 nm with a corresponding band gap of 2.95 eV. These results are in agreement with the literature [14]. Four obvious absorption peaks at 297, 538, 590, and 752 nm indicate UV and visible light absorption. To explain the absorption spectrum, the electronic properties of $NdVO_4$ were calculated with the Vienna *ab initio* simulation package (VASP) on the basis of density functional theory (DFT) using the pseudopotential plane-wave method [17,18]. The density of states (DOSs) and the partial density of states (PDOSs) of $NdVO_4$ crystals are shown in the Fig. 3b. From the PDOSs, the bottom of the conduction band is mainly formed by Nd 4f states and the upper valence band is formed by O 2p states. The calculated band gap (2.9 eV) of the $NdVO_4$ nanowires is smaller than the experimental results. The absorption peak at 297 nm (4.2 eV) is most likely a result of the electron transition in VO_4^{3-}, which corresponds to electron transition from O 2p nonbonding states to V 3d and O 2p antibonding states [19–21]. The absorption peaks at 538 nm (2.3 eV), 590 nm (2.1 eV), and 752 nm (1.6 eV) mainly arise from the electron transition of Nd^{3+}, which corresponds to the 4f electron transitions from $^4I_{9/2}$ to $^2G_{7/2}$, $^4G_{5/2}$, and $^4F_{7/2}$ [3,12,22], as shown in the inset of Fig. 3a. The strong absorption in the UV and visible region facilitates photocatalytic degradation of organic pollutants.

To explore catalytic activity of the $NdVO_4$ nanowires, we performed a degradation experiment of RhB under irradiation of 100 mW/cm^2 simulated sunlight. The characteristic absorption peak of RhB centered at 550 nm was monitored to track the degradation of RhB. Fig. 4a shows the UV–vis absorption spectrum of the starting solution (0.01 mmol/L RhB) and the solution containing 0.2 g/L $NdVO_4$ nanowires as a function of time. Approximately 9% of RhB was adsorbed on the surface of $NdVO_4$ nanowires in the initial 1 h stirring in dark conditions. After illumination, the concentration of RhB decreases with increasing illumination time. To clearly illustrate the degradation rate, we plotted the catalytic degradation percentage versus illumination time in Fig. 4b. The degradation rate is 15%/h in the first hour of illumination, and then slows to 11%/h in the second hour. The degradation rate becomes a constant of 8%/h after 2 h illumination. About 66% of RhB can be effectively degraded by the catalysis of $NdVO_4$ nanowires within 6 h.

The mechanism of the photocatalytic reaction can be described as follows: the photogenerated electron (e^-), and hole (h^+) pairs of the photocatalyst are generated under light excitation (absorbed energy is equal to or larger than its band gap). Then, these electrons and holes react with species adsorbed to the surface, like O_2, OH^-, etc., to form reactive species O_2^-, ·OH. These reactive species degrade the RhB into small molecules like CO_2, H_2O, etc. [23].

Generally, two mechanisms are involved in the degradation of RhB. The de-ethylation and the cleavage of conjugated chromophore structure, which can be characterized by the shift of the maximum absorption band (λ_{max}) and by the change in the absorption maximum (A_{max}/A^0_{max}) of RhB respectively [24,25]. Usually these two mechanisms take place simultaneously and competitively in the photocatalysis process. In Fig. 4a, a change in the absorption maximum can be observed but not a shift of the maximum absorption band. This indicates that the cleavage of the

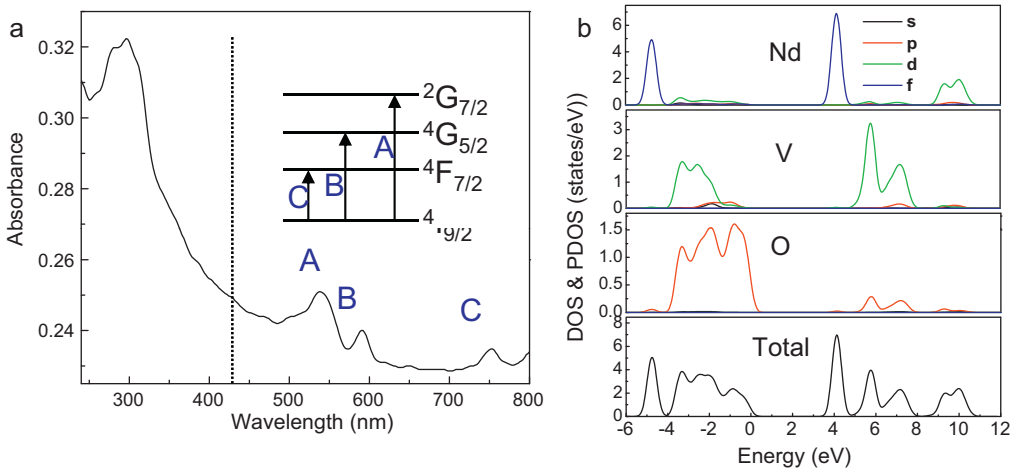

Fig. 3. UV–vis absorption spectrum of the $NdVO_4$ nanowires (a), a schematic diagram of the energy levels responsible for the different peaks (inset), and density of states (DOSs) and partial density of states (PDOSs) of $NdVO_4$ (b).

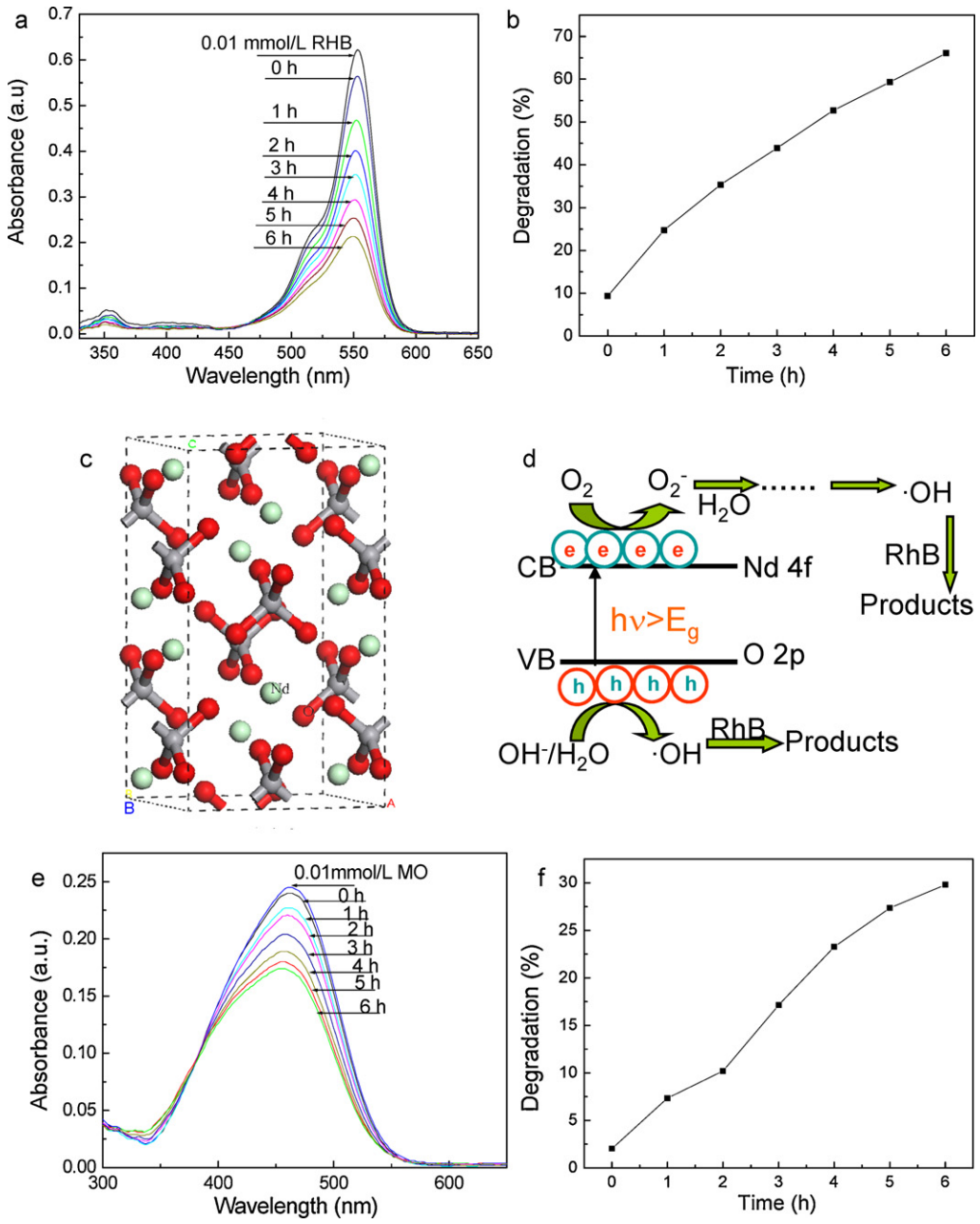

Fig. 4. Absorption spectrum of 0.01 mmol/L RhB (a) and MO (e) solution with 0.2 g/L $NdVO_4$ nanowires in different stages of illumination, the plots of degradation percentage versus illumination time for RhB (b) and MO (f), crystal structure schematic sketch of $NdVO_4$ nanowires (c) and schematic diagram for transfer of electrons in $NdVO_4$ nanowires under visible light irradiation (d).

conjugated chromophore structure by hydroxylation was the dominant mechanism in the photocatalysis. The possible photocatalytic reaction in the visible light/$NdVO_4$ system is proposed as follows:

$$NdVO_4 + hv \rightarrow NdVO_4 + h^+ + e^-,$$

$$H_2O + h^+ \rightarrow OH^- + H^+,$$

$$OH^- + h^+ \rightarrow \cdot OH,$$

$$O_2 + e^- \rightarrow \cdot O_2^-,$$

$$H_2O + \cdot O_2^- \rightarrow \cdot OOH + OH^-,$$

$$2\cdot OOH \rightarrow O_2 + H_2O_2,$$

$$\cdot OOH + H_2O + e^- \rightarrow H_2O_2 + OH^-,$$

$$H_2O_2 + e^- \rightarrow \cdot OH + OH^-,$$

$$RhB + \cdot OH \rightarrow CO_2 + H_2O + NO_3^- + NH_4^+.$$

The regular VO_4 tetrahedra and Nd^{3+} of $NdVO_4$ play a crucial role in the photocatalytic process. Fig. 4c shows the structure schematic of $NdVO_4$ nanowires, indicating the crystal structure of VO_4 tetrahedral and isolated Nd cations. The VO_4 and the Nd cations are alternately stacked in layers orientated along [−1 1 1] direction, which is consistent with results from HRTEM image in Fig. 2d. Thus, the VO_4 tetrahedra interact strongly with each other along the VO_4 chains. The high photocatalytic activity in $NdVO_4$ nanowires is observed partly due to the presence of regular VO_4 tetrahedra and

the layered structure, both of which are beneficial for the charge transfer to the surface [15,26,27]. The UV–vis spectrum shows that Nd^{3+} can absorb visible light energy effectively for 4f electron transition. The transitions of 4f electrons lead to the enhancement of the visible light adsorption of the catalyst and promote the separation of photo-generated electron–hole pairs [8,10], as illustrated in Fig. 4d.

Additionally, a high degree of crystallinity and large surface to volume ratio can improve the activity of the photocatalyst [10,28,29]. The results of XRD and SEAD reveal few grain boundaries within the $NdVO_4$ nanowires due to the degree of crystallinity. These grain boundaries serve as a recombination center between photogenerated electrons and holes [28,30]. In addition, the needle-like $NdVO_4$ nanowires provide a large surface to volume ratio. As a general rule, smaller nanostrucutres allow for more efficient transfer of electron–hole pairs generated from inside the crystal to the surface. A large surface area not only supplies more active sites for the degradation reaction of the dyes but also effectively promotes the separation of the electron–hole pairs, resulting in a higher efficiency of the photocatalytic reaction [11,29].

To explore catalytic selectivity of $NdVO_4$ nanowires, we performed the degradation experiment of methyl orange (MO) solution (yellow) under the same condition. In Fig. 4e and f, about only 29.8% of MO can be effectively degraded by the catalysis of $NdVO_4$ nanowires within 6 h, which indicates that $NdVO_4$ nanowires are more suitable for degradation of RhB.

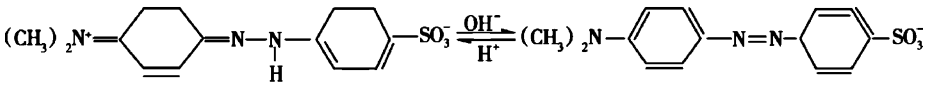

red (quinoid, $ArSO_3$) yellow (azo, $ArSO_3^-$)

From the above reaction equation, the exiting form of MO is mainly $ArSO_3^-$ anion which results in the yellow color of the solution. According to known adsorption mechanisms of $ArSO_3^-$ on catalysts [31,32], the $ArSO_3^-$ anion will partially substitute OH^- adsorbed on the surface of the catalyst in the photocatalysis process. This leads to the decrease of ·OH radicals. Thus, the photocatalytic degradation efficiency of MO is lower than that of RhB under the same conditions.

4. Conclusions

$NdVO_4$ nanowires have been synthesized by the newly developed one-step CMS method. The $NdVO_4$ nanowires show strong UV and visible light absorption. Under visible light irradiation, about 66% of RhB can be effectively degraded by the catalysis of $NdVO_4$ nanowires over 6 h of illumination. This degradation can be attributed to the electron transitions of 4f electrons, the regular VO_4 tetrahedra, the high degree of crystallinity, and the small size and large surface to volume ratio of the $NdVO_4$ nanowires. This study presents a new synthesis method for $NdVO_4$ nanowires and gives a better understanding of the band structure of $NdVO_4$ and photocatalytic mechanism. Excellent catalytic degradation activity of the $NdVO_4$ nanowires suggests possible applications in organic pollutant treatment under visible light irradiation.

Acknowledgments

This work is financially supported by the NSFC (60976055), NSFDYS (50925205), and Postgraduates' Innovative Training Project (S-09109) of the 3rd-211 Project, and the large-scale equipment sharing fund of Chongqing University. The authors thank Dr. Bryan Baker in MSE of Georgia Tech for English language editing.

References

[1] W.M. Hou, Y. Ku, J. Alloys Compd. 509 (2011) 5913–5918.
[2] Y.H. Xu, C. Chen, X.L. Yang, X. Li, B.F. Wang, Appl. Surf. Sci. 225 (2009) 8624–8628.
[3] V. Stengle, S. Bakardjieva, N. Murafa, Mater. Chem. Phys. 114 (2009) 217–226.
[4] C. Wang, Y.H. Ao, P.F. Wang, J. Hou, J. Qian, Appl. Surf. Sci. 257 (2010) 227–231.
[5] Y. Liu, F. Xin, F.M. Wang, S.X. Luo, X.H. Yin, J. Alloys Compd. 498 (2010) 179–184.
[6] G. Liu, G.S. Li, X.Q. Qiu, L.P. Li, J. Alloys Compd. 481 (2009) 492–497.
[7] R. Chen, Z.R. Shen, H. Wang, H.J. Zhou, Y.P. Liu, D.T. Ding, T.H. Chen, J. Alloys Compd. 509 (2011) 2588–2596.
[8] D. Zhao, T.Y. Peng, J.R. Xiao, C.H. Yan, X.Z. Ke, Mater. Lett. 61 (2007) 105–110.
[9] C.M. Huang, G.T. Pan, Y.C.M. Li, M.H. Li, T.C.K. Yang, Appl. Catal. A 358 (2009) 164–172.
[10] Y. Shen, M.L. Huang, Y. Huang, J.M. Lin, J.H. Wu, J. Alloys Compd. 496 (2010) 287–292.
[11] F.X. Wang, M.W. Shao, L. Cheng, J. Hua, X.W. Wei, Mater. Res. Bull. 44 (2009) 1687–1691.
[12] J.W. Shur, V.V. Kochurikhin, A.E. Borisova, M.A. Ivanov, D.H. Yoon, Opt. Mater. 26 (2004) 347–350.
[13] X.C. Wu, Y.R. Tao, L. Dong, J.J. Zhu, Z. Hu, J. Phys. Chem. B 109 (2005) 11544–11547.
[14] S. Mahapatra, G. Madras, T.N.G. Row, Ind. Eng. Chem. Res. 46 (2007) 1013–1017.
[15] S. Mahapatra, S.K. Nayak, G. Madras, T.N.G. Row, Ind. Eng. Chem. Res. 47 (2008) 6509–6516.
[16] X. Wang, C.G. Hu, H. Liu, G.J. Du, X.S. He, Y. Xi, Sens. Actuators, B 144 (2010) 220–225.
[17] G. Kresse, J. Furtműller, Comput. Mater. Sci. 6 (1996) 15–50.
[18] G. Kresse, J. Furtműller, Phys. Rev. B 654 (1996) 11169–11186.
[19] K. Riwotzki, M. Hassse, J. Phys. Chem. B 102 (1998) 10129–10135.
[20] M.R. Dolgos, Al.M. Paraskos, M.W. Stoltzfus, S.C. Yarnell, P.M. Woodward, J. Solid State Chem. 182 (2009) 1964–1971.
[21] J. Ma, Q.S. Wu, Y.P. Ding, J. Nanopart. Res. 10 (2008) 775–786.
[22] A. Benayas, D. Jaque, S.J. Hettrick, J.S. Wilkinson, D.P. Shepherd, J. Appl. Phys. 103 (2008) 103104-1–103104-6.
[23] L.L. Ren, Y.P. Zeng, D.L. Jiang, Catal. Commun. 10 (2009) 645–649.
[24] W. Zhao, C. Chen, X. Li, J. Zhao, J. Phys. Chem. B 106 (2002) 5022–5028.
[25] Z.J. Zhang, W.Z. Wang, M. Shang, W.Z. Yin, Catal. Commun. 11 (2010) 982–986.
[26] D. Saha, S. Mahapatra, T.N.G. Row, G. Madras, Ind. Eng. Chem. Res. 48 (2009) 7489–7497.
[27] F. Amano, T. Yamaguchi, T. Tanaka, Catal. Today 120 (2007) 126–132.
[28] X.X. Hu, C. Hu, J.H. Qu, Mater. Res. Bull. 43 (2008) 2986–2997.
[29] J. Shi, S.X. Shang, L. Yang, J.C. Yan, J. Alloys Compd. 479 (2009) 436–439.
[30] R. Konta, H. Kato, H. Kobayashi, A. Kudo, Phys. Chem. Chem. Phys. 5 (2003) 3061–3065.
[31] T.Y. Wei, C.C. Wan, Ind. Eng. Chem. 30 (1991) 1293–1296.
[32] R.W. Matthews, J. Phys. Chem. 91 (1987) 3328–3333.